공학석사 학위논문

Machine Learning Model to Predict Phenoconversion Time and Subtype of Synucleinopathy from Isolated REM Sleep Behavior Disorder using EEG

뇌파를 이용한 단독 렘수면행동장애의 시누클레인병증 발병 시기 및 아형 예측을 위한 기계 학습 모델

2023년 02월

서울대학교 대학원

협동과정 바이오엔지니어링 전공

정 엘

Machine Learning Model to Predict Phenoconversion Time and Subtype of Synucleinopathy from Isolated REM Sleep Behavior Disorder using EEG

지도 교수 정 기 영

이 논문을 공학석사 학위논문으로 제출함
2023년 02월

서울대학교 대학원
협동과정 바이오엔지니어링 전공
정 엘

정엘의 공학석사 학위논문을 인준함
2023년 02월

위 원 장 김 만 호 (인)

부위원장 정 기 영 (인)

위 원 김 한 준 (인)

Abstract

Objective: Isolated rapid eye movement sleep behavior disorder (iRBD) is a prodromal disease of α-synucleinopathies, and more than 80% of cases eventually convert to neurodegenerative diseases including Parkinson's disease (PD), dementia with Lewy bodies (DLB) and multiple system atrophy (MSA). Baseline resting-state electroencephalography (EEG) was reported to be associated with the phenoconversion. This study aimed to develop a prediction model for α-synucleinopathy phenoconversion time and subtype using EEG at baseline in iRBD.

Methods: At baseline, resting-state EEG and neurological assessments were performed on patients with iRBD. EEG spectral power, weighted phase lag index and Shannon entropy were used as features. Three models were used for survival prediction, and four models were applied for subtype prediction to PD-MSA and DLB. In addition, external validation was performed.

Results: 233 patients were followed-up for up to nine years (mean 4.1 years), and 29 converted to α-synucleinopathies (14 PD, 9 DLB, 6 MSA). The best model for survival prediction was the random survival forest with an integrated Brier score of 0.113 and a concordance index of 0.721. K-nearest neighbor was the best model for the subtype prediction with an area under the receiver operating characteristic curve of 0.908. Features related to EEG slowing showed high importance in both models.

Conclusions: Machine learning models using EEG biomarker can be able to predict phenoconversion time and subtype in iRBD. Further study including large sample data from various countries is needed to corroborate our results.

Keyword : REM sleep behavior disorder; Parkinson' s disease; Dementia with Lewy bodies; Multiple system atrophy; EEG; Machine learning.
Student Number : 2020-25765

Table of Contents

List of Tables

List of Figures

Abbreviations

REM, rapid eye movement

RBD, REM sleep behavior disorder

iRBD, isolated RBD

PD, Parkinson's disease

DLB, dementia with Lewy bodies

MSA, multiple system atrophy

EEG, electroencephalogram

PET, positron emission tomography

SPECT, single photon emission computed tomography

fMRI, functional magnetic resonance imaging

RBDQ-KR, Korean version of the RBD Screening Questionnaire-Hong Kong

ICSD-3, International Classification of Sleep Disorders – third edition

vPSG, video-polysomnography

K-MMSE, Korean version of the Mini-Mental Status Examination

MoCA-K, Korean version of the Montreal Cognitive Assessment

KVSS, Korean Version of Sniffing Sticks

SCOPA-AUT, Scales for Outcomes in Parkinson's Disease for Autonomic Symptoms

UPDRS, Unified Parkinson's Disease Rating Scale

PSQI, Pittsburgh Sleep Quality Index

ESS, Epworth Sleepiness Scale

iRBD−C, iRBD converters

iRBD−NC, iRBD nonconverters

IRB, Institutional Review Board

ICA, Independent component analysis

FFT, fast Fourier transforms

DOF, dominant occipital frequency

STF, slow−to−fast power ratio

wPLI, weighted phase lag index

SE, Shannon entropy

CPH, Cox proportional hazard

wAFT, Weibull−accelerated failure time

RSF, random survival forest

C−index, concordance−index

IBS, integrated Brier score

SMOTE, synthetic minority oversampling technique

XGBoost, extreme gradient boosting

RF, random forest

LR, logistic regression

KNN, K−nearest neighbor

AUC, area under the receiver operating characteristic curve

ROC, receiver operating characteristic curve

SNUH, Seoul National University Hospital

UniGe, University of Genoa

DAT-SPECT, dopamine transporter single photon emission tomography

dnPDRBD-RP, de novo Parkinson's disease with a premorbid history of REM sleep behavior disorder-related pattern

Chapter 1. Introduction

Rapid eye movement (REM) sleep behavior disorder (RBD) is characterized by dream enactment and loss of muscular atonia during sleep.[1] Isolated RBD (iRBD) is known as a prodromal disease of α-synucleinopathies, specifically Parkinson's disease (PD), dementia with Lewy bodies (DLB) and multiple system atrophy (MSA).[2,3] According to previous studies, the risk of developing α-synucleinopathy among iRBD patients is approximately 18-25% after three years, 31-41% after five years, 60-76% after ten years and 81-91% after 14 years.[2,4,5] Therefore, it can be interpreted that most of iRBD patients eventually develop α-synucleinopathy.

Clinical, neuroimaging and neurophysiological risk factors for phenoconversion in iRBD patients have been reported. Age, olfactory functions, cognitive functions and motor functions were reported as clinical risk factors.[6–8] Studies using both resting-state and sleep electroencephalogram (EEG) have suggested that EEG slowing can be a potential risk factor in predicting phenoconversion.[9,10] In addition, altered EEG functional connectivity was shown in iRBD patients, and these alterations showed a correlation between the RBD questionnaire scores.[11–13]

Describing the phenoconversion of iRBD patients only with binary data (converted or not) is insufficient because most of iRBD patients are known to eventually progress to neurodegenerative disease. Therefore, the time of conversion should also be provided for patients with iRBD. Additionally, since the α-synucleinopathies have different subtypes, i.e., PD-MSA or DLB, it should also include subtype information. Machine learning is being extensively explored for potential applications in various diseases and has achieved excellent performance compared with conventional methods.[14] Thus, machine learning methods should be considered to predict survival time and subtype class.

We used resting-state EEG to predict phenoconversion time

and subtype in iRBD patients. EEG is a non-invasive, objective and economic method for measuring functional brain state. Compared to clinical features such as olfactory function, constipation and so on, EEG provides objective measurement of brain activity. It is safe and cost effective compared with functional neuroimaging modalities. Nevertheless, EEG based machine learning prediction of phenoconversion has not been studied in iRBD.

The aim of this study was to propose machine learning models that provide a survival function for phenoconversion and predict the subtype of phenoconversion for each patient using baseline EEG data. Therefore, we applied and compared various survival analyses and classification models to select the best model for predicting phenoconversion time and subtype of α-synucleinopathy.

Chapter 2. Materials and methods

2.1. Participants

Patients with iRBD who visited the sleep clinic of Seoul National University Hospital were enrolled in this study, and clinical follow-up was performed each year. The International Classification of Sleep Disorders (ICSD-3) criteria were used to diagnose RBD by overnight video-polysomnography (vPSG).[15] Participants who had a neurodegenerative disease, neurological disorder, severe medical illness or severe obstructive sleep apnea (apnea-hypopnea index ≥ 30) were excluded. Age- and sex-matched healthy volunteers served as healthy controls.

At baseline, two neurologists specialized in sleep disorders (JK) and movement disorders (KH) examined each patient to evaluate for dementia, cerebellar ataxia, parkinsonism or other neurodegenerative diseases.

The Korean version of the Mini-Mental Status Examination (K-MMSE) and the Korean version of the Montreal Cognitive Assessment (MoCA-K) were used to evaluate general cognitive function.[16,17] The Korean version of the RBD Screening Questionnaire-Hong Kong (RBDQ-KR) was used to assess the RBD symptom severity.[18] The Korean Version of Sniffing Sticks (KVSS) was applied to test olfactory symptoms.[19] The Scales for Outcomes in Parkinson's Disease for Autonomic Symptoms (SCOPA-AUT) questionnaire was used to examine the symptoms of autonomic dysfunction.[20] The Unified Parkinson's Disease Rating Scale (UPDRS) part III was used to assess motor symptoms.[21] Additionally, subjective sleep quality and excessive daytime sleepiness were assessed using the Pittsburgh Sleep Quality Index (PSQI) and the Epworth Sleepiness Scale (ESS), respectively.[22,23]

During the follow-up period, motor function and autonomic function (UPDRS part III, SCOPA-AUT), questionnaires for sleep

(PSQI, ESS), RBD symptom severity (RBDQ-KR) and olfactory function (KVSS) were evaluated every 12 months. For the cognitive tests, K-MMSE and MoCA-K were assessed yearly. Phenoconversion was assessed in iRBD patients every 6 to 12 months by the same two neurologists as at baseline. Finally, patients with iRBD who developed PD, DLB or MSA were classified as converters (iRBD-C), while the remaining patients were classified as nonconverters (iRBD-NC). The diagnosis of PD, DLB and MSA was made according to standard criteria.[24–26]

This study was authorized by the Institutional Review Board (IRB) of the Seoul National University Hospital (IRB Number 1406-100-589). In addition, the participants' written informed consent was obtained.

For external validation, clinical and EEG data of iRBD patients were provided by the University of Genoa. Data acquisition for clinical and EEG was described elsewhere.[27] All patients completed routine clinical follow-ups during which systematic assessment for parkinsonism and dementia was performed, including a semistructured interview with patients and caregivers (IRB Number 703, from the Genoa IRB).

2.2. EEG recordings and preprocessing

Scalp EEGs were obtained using an EEG cap (Wave-Guard EEG cap, Advanced NeuroTechnology, Enschede, Netherlands) from 60 electrodes according to the international 10-10 system. The reference electrode was positioned on an ear, whereas the ground electrode was placed on the AFz. Impedances were kept under 10 kΩ. To detect and eliminate eye movement artifacts, two EOG channels were attached to the left and right outer canthi. The signal sampling rate was 400 Hz. The resting-state EEG of all participants was recorded for a total of 5 minutes while they were awake and alternating opening and closing their eyes every 30 seconds. A high-pass filter of 0.5 Hz and a notch filter of 60 Hz was applied. Only EEG data for eyes closed were extracted and

analyzed in this study. EEG segments with severe artifacts or poor signal quality were removed by visually inspecting the data. Then, independent component analysis (ICA) was applied, and the EEGLAB plugin ICLabel was used to automatically remove eye artifacts.[28,29] The threshold for eye artifact probability was set to 90%.

For the external validation set, 61 electrodes were used to record EEG. The reference electrode was placed on an ear, and the signals were sampled at 512 Hz. The acquisition protocol consisted of approximately 25 resting states subdivided into 2–3 minutes with eyes open, 3–4 minutes during hyperventilation and 17–18 minutes with eyes closed. The same preprocessing procedure as in our dataset was implemented in the external validation set.

For both centers' data, a total of 101 seconds of EEG data for each patient were eventually included in this study. EEG preprocessing was performed using EEGLAB version 2019.1, operated in MATLAB (version 9.8.0, The MathWorks, Natick, MA, USA).[30]

2.3. Experimental procedures

2.3.1. EEG features

Since the patient sample size was relatively small to apply machine learning methods, data augmentation was performed for the training set. To augment the total data size, the first 100 two-second EEG epochs were extracted by sliding window method with 50% overlap for each patient. Thus, one patient's EEG data from the training set were augmented to one hundred EEG epochs.

For each EEG epoch, fast Fourier transforms (FFT) using the Hanning window were applied with a frequency of interest range of 1–50 Hz in 0.5 Hz steps. In our study, four frequency bands were used: delta (2–3.5 Hz), theta (4–7.5 Hz), alpha (8–12.5 Hz) and beta (13–30 Hz). Absolute power was averaged across all electrodes and converted to decibel scale. Relative power was

calculated by expressing the percentage of each frequency band over the total power in a range of 2–30 Hz. The dominant occipital frequency (DOF) was defined as the averaged peak frequency in two occipital channels (O1, O2) where the power is maximum between 4–14 Hz. The slow–to–fast power ratio (STF) using absolute power values averaged in all electrodes was calculated as follows: [(delta + theta)/(beta)]. In addition, overall functional connectivity for each frequency band was extracted by averaging the weighted phase lag index (wPLI) values of all 1770 electrode pairs.[11,31] Furthermore, Shannon entropy (SE) was defined with 10 bins of amplitude values.[32] In total, 15 EEG features were calculated for analysis (Table 1). All spectral analyses were performed using the FieldTrip toolbox version 20200607.[33]

Table 1. EEG features

Categories	Features
Frequency-domain	Absolute delta power: 2-3.5 Hz
	Absolute theta power: 4-7.5 Hz
	Absolute alpha power: 8-12.5 Hz
	Absolute beta power: 13-30 Hz
	Relative delta power: 2-3.5 Hz
	Relative theta power: 4-7.5 Hz
	Relative alpha power: 8-12.5 Hz
	Relative beta power: 13-30 Hz
	DOF: occipital peak frequency
	Slow-to-fast power ratio: (delta + theta) / beta
Functional connectivity	Delta wPLI value
	Theta wPLI value
	Alpha wPLI value
	Beta wPLI value
Entropy	Shannon entropy: 10 bins of amplitude

Abbreviations: DOF, dominant occipital frequency; wPLI, weighted phase lag index.

2.3.2. Survival prediction of phenoconversion

Eighty percent of the overall dataset was assigned as a training set, and the remaining 20% of the data were designated as a testing set. All iRBD patient data, which were divided into iRBD-NC and iRBD-C, were used in this survival prediction analysis. Feature selection was performed from the training set by univariable Cox proportional hazard (CPH) regression and backward multivariable CPH regression by eliminating features with a $p > 0.1$. The synthetic minority oversampling technique (SMOTE) resampling were applied in the training set due to the data imbalance.[34] CPH, Weibull-accelerated failure time (wAFT) and random survival forest (RSF) model were used to train and test these data. To evaluate the models, stratified group 5-fold cross-validation was implemented for internal validation. Harrel's concordance index (C-index) and the integrated Brier score (IBS) were used to evaluate the performance of survival prediction analysis.[35,36] For all models, hyperparameter optimization was performed using the training set while the testing set was used for model performance. The final model was fitted with the augmented and resampled total dataset by using the best prediction model. As there were no MSA patients in external validation set, we additionally fitted the model excluding the MSA patients. All analyses were conducted using Python 3.8.5 (scikit-learn: v.1.1.1; lifelines: v.0.27.0; scikit-survival: v.0.18.0; hyperopt: v.0.2.7).

2.3.3. Subtype prediction of phenoconversion

Only iRBD-C data were used for subtype prediction analysis to classify subtypes of phenoconversion. A training set made up of 80% of the dataset and a testing set using the remaining 20% were assigned. In our cohort, a relatively high proportion of patients were converted to MSA (21%), and their EEG spectral characteristics were similar to that of PD (Figure 1 and Table 2), therefore patients with PD and MSA were grouped into PD-MSA subgroup.

The remaining patients were consisted of DLB subgroup. To select features for this analysis, recursive feature elimination by extreme gradient boosting (XGBoost) model was used. Due to data imbalance, the SMOTE resampling technique was applied in the training set. The data were trained and tested using the XGBoost, random forest (RF), logistic regression (LR) with elastic net regularization and k-nearest neighbor (KNN) models. Hyperparameter optimization was performed using the training set for all models while evaluating by the testing set. 10-fold cross-validation was performed repeatedly 10 times for internal validation to assess the models. Area under the receiver operating characteristic curve (AUC), accuracy, precision, recall and F1 score were utilized to evaluate the performance of the subtype prediction analysis. The best prediction model was used to fit the final model to the augmented and resampled entire dataset. For the same reason as in survival prediction, dataset without MSA was additionally analyzed. Classifying into all three subtypes was also done. Python 3.8.5 was used to conduct each and every analysis (scikit-learn: v.1.1.1; xgboost: v.0.90; hyperopt: v.0.2.7).

Figure 1. Power spectral density of HC, PD, DLB and MSA

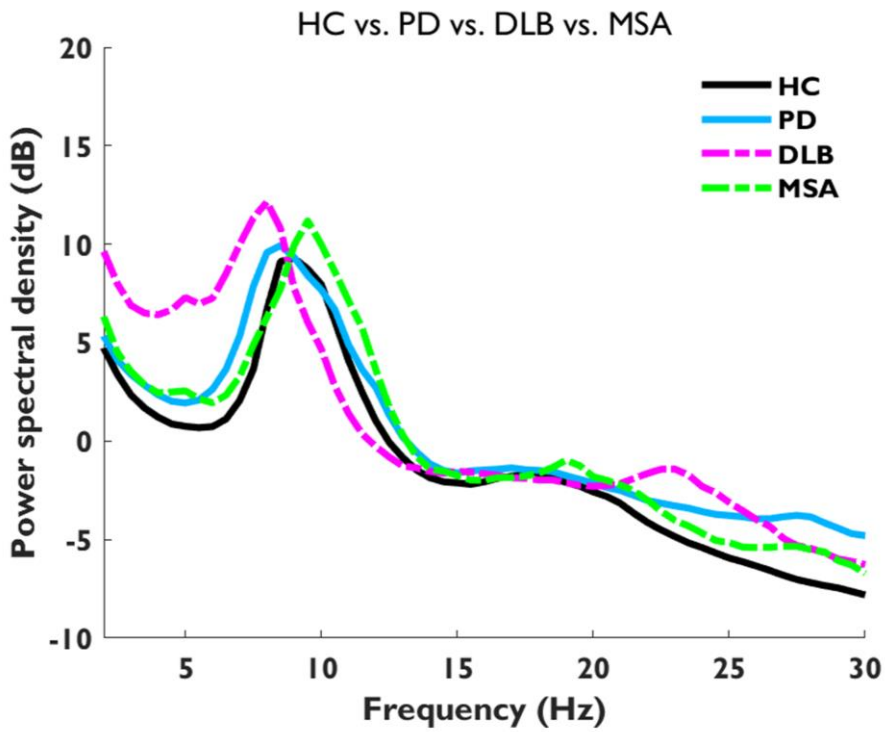

Abbreviations: HC, healthy control; PD, Parkinson's disease; DLB, dementia with Lewy bodies; MSA, multiple system atrophy

Table 2. EEG features of HC, iRBD−NC, PD, MSA and DLB

	HC (n = 51)	iRBD-NC (n = 116)	PD (n = 13)	MSA (n = 6)	DLB (n = 8)
Absolute delta power (dB)	5.04 ± 2.01	4.59 ± 2.27	5.82 ± 1.77	5.93 ± 2.88	8.27 ± 3.90
Absolute theta power (dB)	3.05 ± 2.89	2.77 ± 3.15	5.55 ± 2.65	4.29 ± 3.60	9.36 ± 4.08
Absolute alpha power (dB)	6.84 ± 4.45	6.08 ± 4.45	8.74 ± 3.34	9.22 ± 4.04	8.67 ± 3.19
Absolute beta power (dB)	-1.62 ± 2.63	-1.77 ±2.65	-0.49 ± 2.39	-0.36 ± 1.95	-0.74 ± 3.36
Relative delta power	0.31 ± 0.13	0.32 ± 0.11	0.25 ± 0.09	0.26 ± 0.09	0.28 ± 0.12
Relative theta power	0.18 ± 0.06	0.20 ± 0.06	0.23 ± 0.09	0.17 ± 0.05	0.35 ± 0.10
Relative alpha power	0.45 ± 0.17	0.42 ± 0.14	0.46 ± 0.15	0.52 ± 0.13	0.34 ± 0.17
Relative beta power	0.07 ± 0.03	0.07 ± 0.04	0.07 ± 0.06	0.06 ± 0.03	0.04 ± 0.02
DOF (Hz)	9.03 ± 0.78	9.08 ± 0.83	8.85 ± 0.83	9.52 ± 0.86	7.75 ± 0.88
STF	2.07 ± 0.49	3.65 ± 3.95	2.18 ± 0.61	2.01 ± 0.56	2.97 ± 0.64
Delta wPLI	0.31 ± 0.06	0.29 ± 0.07	0.30 ± 0.08	0.27 ± 0.05	0.26 ± 0.04
Theta wPLI	0.31 ± 0.06	0.30 ± 0.07	0.27 ± 0.07	0.27 ± 0.07	0.27 ± 0.06
Alpha wPLI	0.33 ± 0.07	0.32 ± 0.07	0.24 ± 0.06	0.27 ± 0.08	0.27 ± 0.07
Beta wPLI	0.34 ± 0.06	0.31 ± 0.06	0.27 ± 0.06	0.28 ± 0.06	0.27 ± 0.07
Shannon entropy	1.86 ± 0.05	1.85 ± 0.04	1.85 ± 0.05	1.90 ± 0.04	1.91 ± 0.05

Abbreviations: HC, healthy controls; iRBD, Isolated REM sleep behavior disorder; iRBD−NC, iRBD non−converters; PD, Parkinson's disease; MSA, multiple system atrophy; DLB, dementia with Lewy bodies; DOF, Dominant occipital frequency; STF, Slow−to−fast power ratio; wPLI, weighted phase lag index.

2.4. Statistical analysis

All data are shown as the mean ± standard deviation [range]. The Kolmogorov-Smirnov test was used to test the normality of all variables before analysis. Independent sample t tests were employed to evaluate differences in continuous data. The categorical data were analyzed with Fisher's exact test. Nonnormally distributed variables were compared using the Mann-Whitney U test. Survival curves were plotted using the Kaplan-Meier method. The log-rank test was used to compare survival distributions between our dataset and the external validation dataset. The significance threshold was set to 0.05. All statistical evaluations were performed with Python 3.8.5 using 'SciPy' (scipy: v.1.5.2).

Chapter 3. Results

3.1. Participant characteristics

A total of 233 iRBD patients were included in this study. During a mean follow-up duration of 3.4 years [range: 0.7–9.6 years], 29 patients were converted to neurodegenerative diseases, and 204 remained as isolated state of RBD (Figure 2A). Eighty patients who had no baseline EEG and 10 patients' data that were recorded with another EEG system were excluded from the present study. Of remaining 143 patients twenty-seven patients developed phenoconversion during follow-up (13 to PD, 8 to DLB and 6 to MSA). All MSA patients were of the cerebellar type (MSA-C). Demographic characteristics of 51 healthy controls are presented in Table 3.

There were no significant differences in sex, RBDQ-KR, K-MMSE, KVSS, SCOPA-AUT, ESS and PSQI between iRBD-NC and iRBD-C. However, iRBD-C group were older, had lower education levels, lower MoCA-K scores and higher UPDRS-III scores (Table 4). When comparing PD-MSA and DLB, the DLB group was older and had lower K-MMSE and MoCA-K scores (Table 5).

In the external validation dataset, 62 iRBD patients were included (Table 6). Seven patients were excluded: 5 because of poor data quality and 2 because the data were recorded after phenoconversion. 17 iRBD patients were converted (7 to PD and 10 to DLB) during follow-up. Compared to our dataset, the external validation dataset's age, sex, conversion duration and MMSE were significantly different (Table 7). In addition, the log-rank test showed that the two datasets were significantly different in survival rate (Figure 2B, $p < 0.005$).

Figure 2. Flowchart and survival curve

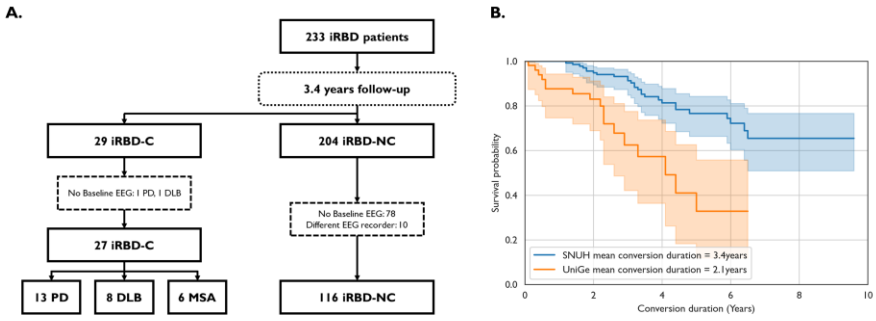

(A) Flowchart. (B) Survival curves of Seoul National University Hospital and University of Genoa. Abbreviations: iRBD, isolated REM sleep behavior disorder; iRBD-C, iRBD converters; iRBD-NC, iRBD nonconverters; PD, Parkinson's disease; DLB, dementia with Lewy bodies; MSA, multiple system atrophy; SNUH, Seoul National University Hospital; UniGe, University of Genoa.

Table 3. Participant characteristics of healthy control from Seoul National University Hospital

	HC (n = 51)
Age (years)	66.22 ± 6.37 [50-77]
Sex (Male %)	M: 35, F: 16 (68.6)
Education (years)	13.69 ± 2.67 [6-19]
MoCA-K	27.33 ± 1.47 [25-30]
KVSS	6.15 ± 0.86 [5-8] (n = 27)
SCOPA-AUT	5.90 ± 4.31 [0-21]

Abbreviations: HC, healthy control; MoCA-K, Korean version of the Montreal Cognitive Assessment; KVSS, Korean Version of Sniffing Sticks; SCOPA-AUT, Scales for Outcomes in Parkinson's Disease for Autonomic Symptoms.

Table 4. Participant characteristics of iRBD patients who further converted or not from Seoul National University Hospital

	iRBD-NC (n = 116)	iRBD-C (n = 27)	p value
Age (years)	66.65 ± 6.42 [50-82]	69.82 ± 7.30 [57-82]	**0.026**
Sex (Male %)	M: 75, F: 41 (64.7)	M: 15, F: 12 (55.6)	0.385[a]
Education (years)	12.85 ± 4.08 [0-18]	10.41 ± 4.41 [0-18]	**0.008**[b]
RBDQ-KR	49.78 ± 19.79 [4-100] (n = 107)	47.65 ± 16.23 [5-70] (n = 23)	0.632
Conversion duration (years)	-	3.39 ± 1.53 [1.2-6.5]	
K-MMSE	27.77 ± 1.77 [21-30]	27.11 ± 2.21 [20-30]	0.130
MoCA-K	25.84 ± 2.78 [16-30]	22.93 ± 4.59 [7-29]	**<0.001**[b]
KVSS	17.36 ± 5.34 [7-31] (n = 105)	18.13 ± 5.96 [7-27] (n = 20)	0.566
SCOPA-AUT	12.56 ± 7.08 [1-30] (n = 108)	15.22 ± 9.06 [2-39] (n = 23)	0.122
UPDRS-III	0.90 ± 1.95 [0-11] (n = 98)	2.88 ± 3.20 [0-9] (n = 17)	**0.001**[b]
ESS	5.60 ± 3.49 [0-16]	6.00 ± 4.18 [1-20]	0.609
PSQI	6.99 ± 4.22 [1-18]	6.37 ± 4.31 [1-18]	0.468

Bold font indicates statistical significance. Abbreviations: iRBD, isolated REM sleep behavior disorder; iRBD-NC, iRBD nonconverters; iRBD-C, iRBD converters; RBDQ-KR, Korean version of the RBD screening Questionnaire-Hong Kong; K-MMSE, Korean version of the Mini-Mental Status Examination; MoCA-K, Korean version of the Montreal Cognitive Assessment; KVSS, Korean Version of Sniffing Sticks; SCOPA-AUT, Scales for Outcomes in Parkinson's Disease for Autonomic Symptoms; UPDRS, Unified Parkinson's Disease Rating Scale; ESS, Epworth Sleepiness Scale; PSQI, Pittsburgh Sleep Quality Index.

a: Fisher's exact test.

b: Mann-Whitney U test.

Table 5. Participant characteristics of iRBD patients who further converted to PD−MSA or DLB from Seoul National University Hospital

	PD-MSA (n = 19)	DLB (n = 8)	p value
Age (years)	67.74 ± 6.55 [57-80]	74.75 ± 6.92 [61-82]	**0.019**
Sex (Male %)	M: 75, F: 41 (64.7)	M: 15, F: 12 (55.6)	0.385[a]
Education (years)	10.68 ± 4.14 [3-16]	9.75 ± 5.26 [0-18]	0.625
RBDQ-KR	48.47 ± 12.00 [19-66] (n = 17)	45.33 ± 26.27 [5-70] (n = 6)	0.694
Conversion duration (years)	3.32 ± 1.30 [1.4-6.0]	3.58 ± 2.08 [1.2-6.5]	0.696
K-MMSE	27.74 ± 1.66 [24-30]	25.63 ± 2.72 [20-28]	**0.020**
MoCA-K	24.32 ± 3.30 [19-29]	19.63 ± 5.71 [7-24]	**0.012**
KVSS	19.18 ± 5.44 [11-27] (n = 14)	15.67 ± 6.92 [7-27] (n = 6)	0.237
SCOPA-AUT	14.83 ± 9.76 [2-39] (n = 18)	16.60 ± 6.58 [9-23] (n = 5)	0.709
UPDRS-III	3.00 ± 3.40 [0-9] (n = 15)	2.00 ± 0.00 [2-2] (n = 2)	0.939[b]
ESS	6.16 ± 4.48 [1-20]	5.63 ± 3.62 [2-13]	0.769
PSQI	6.90 ± 4.16 [2-18]	5.13 ± 4.67 [1-16]	0.339

Bold font indicates statistical significance. Abbreviations: PD, Parkinson's disease; MSA, multiple system atrophy; DLB, dementia with Lewy bodies; RBDQ−KR, Korean version of the RBD screening Questionnaire−Hong Kong; K−MMSE, Korean version of the Mini−Mental Status Examination; MoCA−K, Korean version of the Montreal Cognitive Assessment; KVSS, Korean Version of Sniffing Sticks; SCOPA−AUT, Scales for Outcomes in Parkinson's Disease for Autonomic Symptoms; UPDRS, Unified Parkinson's Disease Rating Scale; ESS, Epworth Sleepiness Scale; PSQI, Pittsburgh Sleep Quality Index.

a: Fisher's exact test.

b: Mann−Whitney U test.

Table 6. Participant characteristics of iRBD patients who further converted or not from University of Genoa

	iRBD-NC (n = 38)	iRBD-C (n = 17)	p value
Age (years)	69.71 ± 6.70 [56-81]	70.94 ± 6.55 [60-84]	0.529
Sex (Male %)	M: 33, F: 5 (86.8)	M: 13, F: 4 (76.5)	0.435[a]
Conversion duration (years)	-	2.05 ± 1.49 [0.1-5.0] (7 PD, 10 DLB)	
MMSE	28.53 ± 1.33 [25-30]	27.06 ± 3.40 [17-30]	0.161[b]
UPDRS-III	1.53 ± 3.72 [0-19] (n = 32)	1.88 ± 2.32 [0-8]	0.101[b]

Abbreviations: iRBD, isolated REM sleep behavior disorder; iRBD-NC, iRBD nonconverters; iRBD-C, iRBD converters; PD, Parkinson's disease; DLB, dementia with Lewy bodies; MMSE, Mini-Mental Status Examination; UPDRS, Unified Parkinson's Disease Rating Scale.

a: Fisher's exact test.

b: Mann-Whitney U test.

Table 7. Participant characteristics of iRBD patients from Seoul National University Hospital and University of Genoa

	SNUH (n = 143)	UniGe (n = 55)	p value
Age (years)	67.81 ± 6.85 [50-82]	69.30 ± 6.28 [57-84]	0.008
Sex (Male %)	M: 90, F: 53 (62.9)	M: 46, F: 9 (83.6)	0.006[a]
Conversion duration (years)	3.39 ± 1.53 [1.2-6.5] (n = 27)	2.05 ± 1.49 [0.1-5.0] (n = 17)	0.007
MMSE	27.82 ± 1.84 [20-30]	27.47 ± 2.68 [17-30]	0.029[b]
UPDRS-III	1.09 ± 2.49 [0-19] (n = 115)	2.62 ± 2.91 [0-9] (n = 49)	0.367[b]

Bold font indicates statistical significance. Abbreviations: SNUH, Seoul National University Hospital; UniGe, University of Genoa; MMSE, Mini−Mental Status Examination; UPDRS, Unified Parkinson's Disease Rating Scale.

a: Fisher's exact test.

b: Mann−Whitney U test.

3.2. Survival prediction

Absolute beta power was excluded through univariable CPH regression, and relative alpha power was further excluded through multivariable CPH regression. Finally, 13 features were included in this survival prediction analysis. The power spectral density of iRBD−NC and iRBD−C are shown in Figure 3A.

We compared the three survival analysis methods using our dataset (Table 8). For the internal validation using 5−fold cross−validation, the RSF model was the best predicting model, with an IBS of 0.113 and a C−index of 0.721. The five most important features of RSF were absolute delta power, absolute theta power, absolute alpha power, STF and beta wPLI (Figure 4 and Table 9). For external validation, the RSF model showed an IBS of 0.136 and a C−index of 0.563. Additionally, evaluations without MSA patients are listed in Table 10.

Figure 3. Power spectral density of participants

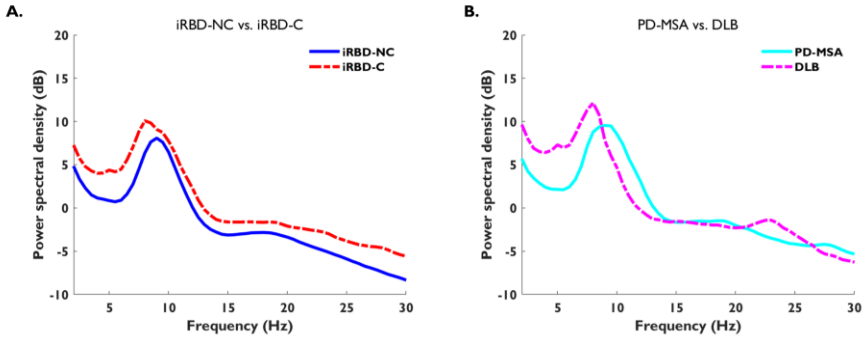

(A) iRBD-NC vs. iRBD-C. (B) PD-MSA vs. DLB. Abbreviations: iRBD, isolated REM sleep behavior disorder; iRBD-C, iRBD converters; iRBD-NC, iRBD nonconverters; PD, Parkinson's disease; DLB, dementia with Lewy bodies; MSA, multiple system atrophy.

Table 8. Survival prediction results

	IBS	C-index
CPH	0.178	0.738
wAFT	0.181	0.729
RSF	0.113	0.721

Abbreviations: IBS, integrated Brier score; C-index, concordance index; CPH, Cox proportional hazard; wAFT, Weibull-accelerated failure time; RSF, random survival forest.

Figure 4. Feature importance of random survival forest model

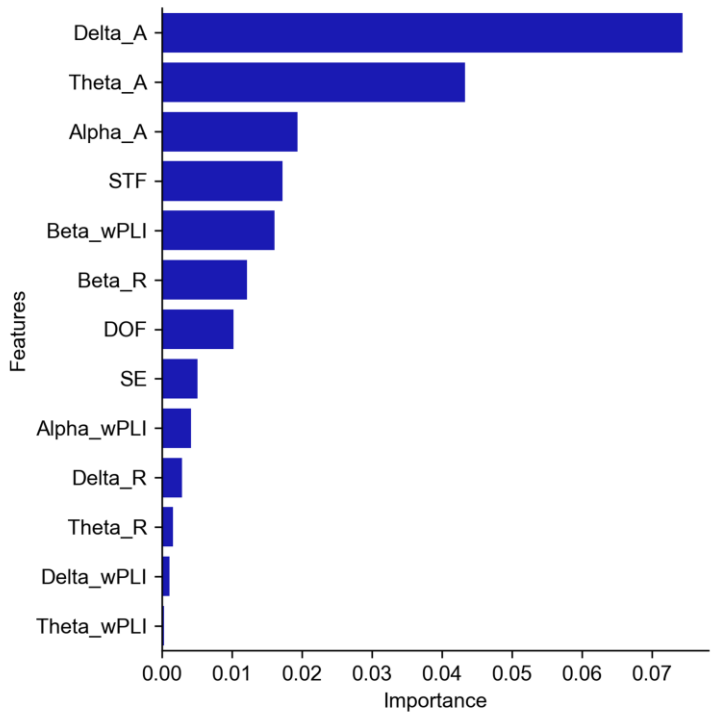

Abbreviations: _A, absolute power; STF, slow-to-fast power ratio; wPLI, weighted phase lag index; SE, Shannon entropy; _R, relative power.

Table 9. Random survival forest model feature importance top 5

	iRBD-NC (n = 116)	iRBD-C (n = 27)	p-value
Absolute delta power (dB)	4.59 ± 2.27	6.57 ± 2.90	**<0.001**
Absolute theta power (dB)	2.77 ± 3.15	6.40 ± 3.78	**<0.001**
Absolute alpha power (dB)	6.08 ± 4.45	8.83 ± 3.33	**0.003**
STF	3.65 ± 3.95	2.38 ± 0.71	0.082
Beta wPLI	0.31 ± 0.11	0.27 ± 0.09	**0.001**

Bold font indicates statistical significance. Abbreviations: iRBD, isolated REM sleep behavior disorder; iRBD−NC, iRBD nonconverters; iRBD−C, iRBD converters; STF, slow−to−fast power ratio; wPLI, weighted phase lag index.
p value: age and sex adjusted by analysis of covariance.

Table 10. Survival prediction results without multiple system atrophy patients

	IBS	C-index
CPH	0.155	0.717
wAFT	0.167	0.722
RSF	0.104	0.709

External validation: RSF IBS: 0.145; C-index: 0.507.

Abbreviations: IBS, integrated Brier score; C-index, concordance index; CPH, Cox proportional hazard; wAFT, Weibull-accelerated failure time; RSF, random survival forest.

3.3. Subtype prediction

Through recursive feature elimination, eight features were excluded due to its low feature importance. As a result, seven features were used in this subtype prediction analysis. The selected features in subtype prediction were DOF, STF, absolute theta and beta power, relative beta power, beta wPLI and Shannon entropy (Table 11). The power spectral density of the PD-MSA and DLB group are shown in Figure 3B.

The scores for internal validation predicting PD-MSA and DLB are shown in Table 12. For internal validation by repeated 10-fold cross-validation, the KNN model's performance was the best among the models, with AUC of 0.908, accuracy of 0.815, precision of 0.636, recall of 0.875 and F1 of 0.737 (Figure 5). External validation using the KNN model scored AUC of 0.505, accuracy of 0.491, precision of 0.261, recall of 0.353 and F1 of 0.300. In addition, evaluation results without MSA patients and classification into three subtypes are shown in Tables 13 and 14, respectively.

Figure 5. K-nearest neighbor model prediction results

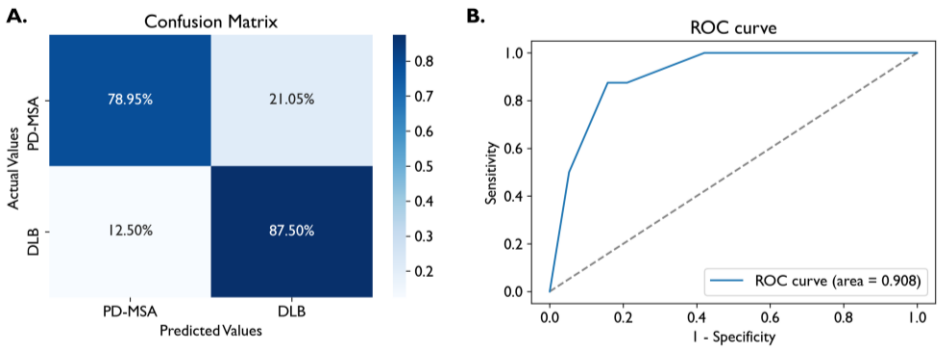

These results are obtained by internal validation using repeated 10-fold cross-validation. (A) Confusion matrix. (B) Receiver operating characteristic curve. Abbreviations: PD, Parkinson's disease; MSA, multiple system atrophy; DLB, dementia with Lewy bodies; ROC, receiver operating characteristic curve.

Table 11. Selected features comparison in subtype prediction

	PD-MSA (n = 19)	DLB (n = 8)	p value
DOF (Hz)	9.07 ± 0.88	7.75 ± 0.88	**0.004**
STF	2.13 ± 0.58	2.97 ± 0.64	**0.001**
Absolute theta power (dB)	5.15 ± 2.94	9.36 ± 4.08	**0.009**
Absolute beta power (dB)	-0.45 ± 2.21	-0.74 ± 3.36	0.648
Relative beta power	0.06 ± 0.05	0.04 ± 0.02	**0.043**
Beta wPLI	0.27 ± 0.06	0.27 ± 0.07	0.266
Shannon entropy	1.85 ± 0.04	1.91 ± 0.05	0.160

Bold font indicates statistical significance. Abbreviations: PD, Parkinson's disease; MSA, multiple system atrophy; DLB, dementia with Lewy bodies; DOF, dominant occipital frequency; STF, Slow-to-fast power ratio; wPLI, weighted phase lag index.
p value: age and sex adjusted by analysis of covariance.

Table 12. Subtype prediction results

	AUC	Accuracy	Precision	Recall	F1
XGBoost	0.803	0.630	0.429	0.750	0.546
RF	0.829	0.741	0.546	0.750	0.642
LR	0.809	0.778	0.600	0.750	0.667
KNN	0.908	0.815	0.636	0.875	0.737

Abbreviations: XGBoost, extreme gradient boosting; RF, random forest; LR, logistic regression; KNN, K−nearest neighbor; AUC, area under the receiver operating characteristic curve.

Table 13. Subtype prediction results without multiple system atrophy patients

	AUC	Accuracy	Precision	Recall	F1
XGBoost	0.7115	0.714	0.625	0.625	0.625
RF	0.7212	0.762	0.714	0.625	0.667
LR	0.7212	0.714	0.667	0.500	0.571
KNN	0.7115	0.714	0.625	0.625	0.625

External validation: RF AUC: 0.499; accuracy: 0.600; precision: 0.381; recall: 0.471; F1: 0.421.

Abbreviations: XGBoost, extreme gradient boosting; RF, random forest; LR, logistic regression; KNN, K−nearest neighbor; AUC, area under the receiver operating characteristic curve.

Table 14. Subtype prediction results into three subtypes (Parkinson's disease, dementia with Lewy bodies, multiple system atrophy)

	Accuracy
XGBoost	0.444
RF	0.444
LR	0.222
KNN	0.482

External validation: KNN accuracy: 0.418.

Abbreviations: XGBoost, extreme gradient boosting; RF, random forest; LR, logistic regression; KNN, K-nearest neighbor.

Chapter 4. Discussion

In this study, we proposed an iRBD phenoconversion time and subtype prediction model using baseline resting-state EEG data. Our model was able to predict the time to conversion and the subtype of phenoconversion. Using RSF model, phenoconversion time was capable of predicting with acceptable performance. In addition, KNN model could predict whether iRBD-C patients will convert to PD-MSA or DLB with good performance.

In our study, we predicted survival rates for phenoconversion in iRBD patients using EEG features alone. Absolute delta, theta and alpha power, STF and beta wPLI were the most important features for survival prediction. In previous studies, it is known that the absolute EEG power was significantly different in both sleep and resting-state not only between iRBD patients and controls, but also between iRBD patients who converted to neurodegenerative diseases and yet converted.[9,10,37–40] In particular, the increase in absolute theta and delta power is prominent in converted patients. A previous study found that the DOF of iRBD-C revealed no difference from that of iRBD-NC.[10] Higher low-frequency power and lower high-frequency power, known as EEG slowing in iRBD patients, have already been shown in various neurodegenerative studies.[10,38,41–43] Therefore, as EEG slowing is known to be common in iRBD patients, particularly in iRBD patients who converted to neurodegenerative diseases, our result suggests that EEG can be applied as a biomarker for predicting phenoconversion in iRBD patients.

Phenoconversion subtype prediction from iRBD patients was also feasible using EEG features. EEG differences between the PD-MSA and DLB were shown in a previous study, indicating that the DLB patients showed increased delta and theta power, higher STF and lower DOF.[10] These findings are explained by EEG slowing, which is more prominent in DLB patients as our study. In addition, EEG slowing is correlated with cognitive impairment.[44] In previous studies comparing the PD-MSA and DLB, the main difference at

baseline was cognitive function, which was significantly decreased in the DLB group.[2,45,46] As a result, the different EEG characteristics of these two groups imply that EEG could be a good tool for differentiating subtypes of iRBD phenoconversion. Indeed, selected features in the subtype prediction were DOF, STF, absolute theta and beta power, which are also in line with previous studies.

Previous studies have been conducted to identify biomarkers that can predict the development of synucleinopathies in patients with iRBD. According to a large multicenter longitudinal study, motor and cognitive measures showed high hazard ratios (up to 3.16 for abnormal quantitative motor testing) as risk factors predicting phenoconversion in patients with iRBD.[2] Another international multicenter study using dopamine transporter single photon emission tomography (DAT-SPECT) suggested a combination of risk factors predicting phenoconversion in iRBD.[47] The best risk factor combination, including age, constipation and putamen dopaminergic dysfunction in the most affected hemisphere, yielded a hazard ratio of 5.71, which was higher than the hazard ratios of clinical features alone. Moreover, de novo PD with a premorbid history of RBD-related pattern (dnPDRBD-RP) was suggested as a biomarker to predict phenoconversion in iRBD patients with a hazard ratio of 8.95.[48] However, as dnPDRBD-RP was solely obtained from PD patients, it did not represent specific metabolic changes related to DLB or MSA. In our study, we showed good performance predicting not only the time, but also the subtype of phenoconversion, by using only resting-state EEG without any clinical or neuroimaging features. As previously mentioned, EEG recording provides benefits over other biomarkers employed in earlier studies, especially in terms of simplicity and cost-effectiveness, so if it is developed as a wearable device that records EEG activity with only a few channels, it can be easily applied in clinical practice.

It is notable that the performance of external validation was poor in both survival prediction and subtype prediction in our research. Compared to the external validation dataset, our dataset

showed a higher female proportion, younger age, lower UPDRS-III score, slower survival rate and more MSA converted patients. These differences might have caused the poor performance in this study. In further research, Asian cohorts should be used for external validation. On the other hand, this could be a result of overfitting to our dataset. However, we validated the results by cross-validation and changed parameters that are known to be related to avoid overfitting.

There are two main strengths of this study. First, this study is the first to predict the phenoconversion time and subtype of synucleinopathy in iRBD patients using baseline EEG data. EEG is easy to record and not expensive compared to other neuroimaging methods and is sensitive to brain functions, stable and the test-retest reliability is high.[49] Second, we not only validated in our dataset but also validated externally. Despite the strengths of this study, there are a few limitations. First, the age and cognitive function scores, which may affect EEG findings were not adjusted.[50,51] Second, due to the small sample size, we had no choice but to apply data augmentation. The number of iRBD patients in this study was 143, which was relatively small for the use of machine learning methods. However, as many studies used EEG sliding window data augmentation, this data augmentation might be reliable enough to achieve the study goal.[52–54]

In conclusion, we could make a useful model with RSF model and KNN model for predicting time of phenoconversion and its subtype respectively in iRBD patients simply using resting-state EEG at baseline. Future multicenter study with larger number of patients is needed to elucidate the predictive value of baseline EEG.

Bibliography

1. Schenck CH, Bundlie SR, Ettinger MG, Mahowald MW. Chronic behavioral disorders of human REM sleep: a new category of parasomnia. *Sleep*. 1986;9(2):293–308. doi:10.1093/sleep/9.2.293

2. Postuma RB, Iranzo A, Hu M, et al. Risk and predictors of dementia and parkinsonism in idiopathic REM sleep behaviour disorder: a multicentre study. *Brain J Neurol*. 2019;142(3):744–759. doi:10.1093/brain/awz030

3. Zhou J, Zhang J, Lam SP, Tang X, Wing YK. Clinical Biomarkers of Neurodegeneration in REM Sleep Behavior Disorder. *J Sleep Med*. 2015;12(2):27–33. doi:10.13078/jsm.15006

4. Iranzo A, Fernández-Arcos A, Tolosa E, et al. Neurodegenerative Disorder Risk in Idiopathic REM Sleep Behavior Disorder: Study in 174 Patients. *PLOS ONE*. 2014;9(2):e89741. doi:10.1371/journal.pone.0089741

5. Postuma RB, Iranzo A, Hogl B, et al. Risk factors for neurodegeneration in idiopathic rapid eye movement sleep behavior disorder: A multicenter study. *Ann Neurol*. 2015;77(5):830–839. doi:10.1002/ana.24385

6. Miglis MG, Adler CH, Antelmi E, et al. Biomarkers of conversion to α-synucleinopathy in isolated rapid-eye-movement sleep behaviour disorder. *Lancet Neurol*. 2021;20(8):671–684. doi:10.1016/S1474-4422(21)00176-9

7. Wang C, Chen F, Li Y, Liu J. Possible predictors of phenoconversion in isolated REM sleep behaviour disorder: a systematic review and meta-analysis. *J Neurol Neurosurg Psychiatry*. 2022;93(4):395–403. doi:10.1136/jnnp-2021-328062

8. de Natale ER, Wilson H, Politis M. Predictors of RBD progression and conversion to synucleinopathies. *Curr Neurol Neurosci Rep*. 2022;22(2):93–104. doi:10.1007/s11910-022-01171-0

9. Gong SY, Shen Y, Gu HY, et al. Generalized EEG Slowing Across Phasic REM Sleep, Not Subjective RBD Severity, Predicts Neurodegeneration in Idiopathic RBD. *Nat Sci Sleep*.

2022;14:407−418. doi:10.2147/NSS.S354063

10. Rodrigues Brazète J, Gagnon JF, Postuma RB, Bertrand JA, Petit D, Montplaisir J. Electroencephalogram slowing predicts neurodegeneration in rapid eye movement sleep behavior disorder. *Neurobiol Aging*. 2016;37:74−81. doi:10.1016/j.neurobiolaging.2015.10.007

11. Sunwoo JS, Lee S, Kim JH, et al. Altered Functional Connectivity in Idiopathic Rapid Eye Movement Sleep Behavior Disorder: A Resting−State EEG Study. *Sleep*. 2017;40(zsx058). doi:10.1093/sleep/zsx058

12. Byun JI, Cha KS, Kim M, et al. Altered insular functional connectivity in isolated REM sleep behavior disorder: a data−driven functional MRI study. *Sleep Med*. 2021;79:88−93. doi:10.1016/j.sleep.2020.12.038

13. Byun JI, Kim HW, Kang H, et al. Altered resting−state thalamo−occipital functional connectivity is associated with cognition in isolated rapid eye movement sleep behavior disorder. *Sleep Med*. 2020;69:198−203. doi:10.1016/j.sleep.2020.01.010

14. Ben−Israel D, Jacobs WB, Casha S, et al. The impact of machine learning on patient care: A systematic review. *Artif Intell Med*. 2020;103:101785. doi:10.1016/j.artmed.2019.101785

15. American Academy of Sleep Medicine. *The International Classification of Sleep Disorders*. 3rd ed. Darien, IL: American Academy of Sleep Medicine; 2014.

16. Lee J young, Lee DW, Cho S jin, et al. Brief screening for mild cognitive impairment in elderly outpatient clinic: Validation of the Korean version of the Montreal cognitive assessment. *J Geriatr Psychiatr Neurol.* 2008;21(2):104e10. https://doi.org/10.1177/0891988708316855

17. Kang YW, Na DL, Hahn SH. A validity study on the korean mini−mental state examination (K−MMSE) in dementia patients. *J Korean Neurol Assoc*. 1997;15(2):300−308.

18. You S, Moon HJ, Do SY, et al. The REM Sleep Behavior Disorder Screening Questionnaire: Validation Study of the Korean Version (RBDQ−KR). *J Clin Sleep Med*. 2017;13(12):1429−1433. doi:10.5664/jcsm.6840

19. Cho JH, Jeong YS, Lee YJ, Hong SC, Yoon JH, Kim JK. The Korean version of the Sniffin' stick (KVSS) test and its validity in comparison with the cross-cultural smell identification test (CC-SIT). *Auris Nasus Larynx*. 2009;36(3):280-286. doi:10.1016/j.anl.2008.07.005

20. Visser M, Marinus J, Stiggelbout AM, Hilten JJV. Assessment of autonomic dysfunction in Parkinson's disease: The SCOPA-AUT. *Mov Disord*. 2004;19(11):1306-1312. doi:10.1002/mds.20153

21. Fahn S, Elton RL. UPDRS program members. Unified Parkinsons disease rating scale. In: Fahn S, Marsden CD, Goldstein M, et al., editors. Recent developments in Parkinsons disease, vol. 2. Florham Park, NJ: Macmillan Healthcare Information; 1987. p. 153-63

22. Johns MW. A new method for measuring daytime sleepiness: the Epworth sleepiness scale. *Sleep*. 1991;14(6):540-545. doi:10.1093/sleep/14.6.540

23. Buysse DJ, Reynolds CF, Monk TH, Berman SR, Kupfer DJ. The Pittsburgh Sleep Quality Index : A New Instrument Psychiatric Practice and Research. *Psychiatry Res*. 1989;28(2):193-231. doi:10.1016/0165-1781(89)90047-4

24. Hughes AJ, Daniel SE, Kilford L, Lees AJ. Accuracy of clinical diagnosis of idiopathic Parkinson's disease: a clinico-pathological study of 100 cases. *J Neurol Neurosurg Psychiatry*. 1992;55(3):181-184. doi:10.1136/jnnp.55.3.181

25. McKeith IG, Dickson DW, Lowe J, et al. Diagnosis and management of dementia with Lewy bodies: Third report of the DLB consortium. *Neurology*. 2005;65(12):1863-1872. doi:10.1212/01.wnl.0000187889.17253.b1

26. Gilman S, Wenning GK, Low PA, et al. Second consensus statement on the diagnosis of multiple system atrophy. *Neurology*. 2008;71(9):670-676. doi:10.1212/01.wnl.0000324625.00404.15

27. Roascio M, Canessa A, Trò R, et al. Phase and amplitude electroencephalography correlations change with disease progression in people with idiopathic rapid eye-movement sleep

behavior disorder. *Sleep*. Published online September 22, 2021:zsab232. doi:10.1093/sleep/zsab232

28. Pion-Tonachini L, Kreutz-Delgado K, Makeig S. ICLabel: An automated electroencephalographic independent component classifier, dataset, and website. *NeuroImage*. 2019;198:181-197. doi:10.1016/j.neuroimage.2019.05.026

29. Jung TP, Makeig S, Humphries C, et al. Removing electroencephalographic artifacts by blind source separation. *Psychophysiology*. 2000;37(2):163-178. doi:10.1111/1469-8986.3720163

30. Delorme A, Makeig S. EEGLAB: an open source toolbox for analysis of single-trial EEG dynamics including independent component analysis. *J Neurosci Methods*. 2004;134:9-21. doi:10.1016/j.jneumeth.2003.10.009

31. Vinck M, Oostenveld R, van Wingerden M, Battaglia F, Pennartz CMA. An improved index of phase-synchronization for electrophysiological data in the presence of volume-conduction, noise and sample-size bias. *NeuroImage*. 2011;55(4):1548-1565. doi:10.1016/j.neuroimage.2011.01.055

32.Shannon, C.E. (1948) A Mathematical Theory of Communication. Bell System Technical Journal, 27, 379-423. doi:10.1002/j.1538-7305.1948.tb01338.x.

33. Oostenveld R, Fries P, Maris E, Schoffelen JM. FieldTrip: Open Source Software for Advanced Analysis of MEG, EEG, and Invasive Electrophysiological Data. *Comput Intell Neurosci*. 2010;2011:e156869. doi:10.1155/2011/156869

34. Chawla NV, Bowyer KW, Hall LO, Kegelmeyer WP. SMOTE: synthetic minority over-sampling technique. *J Artif Intell Res*. 2002;16(1):321-357.

35. Graf E, Schmoor C, Sauerbrei W, Schumacher M. Assessment and comparison of prognostic classification schemes for survival data. Stat Med. 1999;18(17-18):2529-2545. doi:10.1002/(sici)1097-0258(19990915/30)18:17/18<2529::aid-sim274>3.0.co;2-5

36. Harrell FE Jr, Califf RM, Pryor DB, Lee KL, Rosati RA. Evaluating the Yield of Medical Tests. *JAMA*.

1982;247(18):2543–2546.
doi:10.1001/jama.1982.03320430047030

37. Ruffini G, Ibañez D, Castellano M, et al. Deep Learning With EEG Spectrograms in Rapid Eye Movement Behavior Disorder. *Front Neurol*. 2019;10. doi:10.3389/fneur.2019.00806

38. Livia Fantini M, Gagnon JF, Petit D, et al. Slowing of electroencephalogram in rapid eye movement sleep behavior disorder. *Ann Neurol*. 2003;53(6):774–780. doi:10.1002/ana.10547

39. Soikkeli R, Partanen J, Soininen H, Pääkkönen A, Riekkinen P. Slowing of EEG in Parkinson's disease. *Electroencephalogr Clin Neurophysiol*. 1991;79(3):159–165. doi:10.1016/0013-4694(91)90134-P

40. Klassen BT, Hentz JG, Shill HA, et al. Quantitative EEG as a predictive biomarker for Parkinson disease dementia. *Neurology*. 2011;77(2):118–124. doi:10.1212/WNL.0b013e318224af8d

41. Sasai T, Matsuura M, Inoue Y. Electroencephalographic Findings Related With Mild Cognitive Impairment in Idiopathic Rapid Eye Movement Sleep Behavior Disorder. *Sleep*. 2013;36(12):1893–1899. doi:10.5665/sleep.3224

42. Rodrigues Brazète J, Montplaisir J, Petit D, et al. Electroencephalogram slowing in rapid eye movement sleep behavior disorder is associated with mild cognitive impairment. *Sleep Med*. 2013;14(11):1059–1063. doi:10.1016/j.sleep.2013.06.013

43. Iranzo A, Isetta V, Molinuevo JL, et al. Electroencephalographic slowing heralds mild cognitive impairment in idiopathic REM sleep behavior disorder. *Sleep Med*. 2010;11(6):534–539. doi:10.1016/j.sleep.2010.03.006

44. Geraedts VJ, Boon LI, Marinus J, et al. Clinical correlates of quantitative EEG in Parkinson disease: A systematic review. *Neurology*. 2018;91(19):871–883. doi:10.1212/WNL.0000000000006473

45. Terzaghi M, Toscano G, Casoni F, et al. Assessment of cognitive profile as a prodromal marker of the evolution of rapid eye movement sleep behavior disorder. *Sleep*. 2019;42(8).

doi:10.1093/sleep/zsz103

46. Génier Marchand D, Montplaisir J, Postuma RB, Rahayel S, Gagnon JF. Detecting the Cognitive Prodrome of Dementia with Lewy Bodies: A Prospective Study of REM Sleep Behavior Disorder. *Sleep*. 2017;40(1). doi:10.1093/sleep/zsw014

47. Arnaldi D, Chincarini A, Hu MT, et al. Dopaminergic imaging and clinical predictors for phenoconversion of REM sleep behaviour disorder. *Brain*. 2021;144(1):278–287. doi:10.1093/brain/awaa365

48. Shin JH, Lee JY, Kim YK, et al. Parkinson Disease–Related Brain Metabolic Patterns and Neurodegeneration in Isolated REM Sleep Behavior Disorder. *Neurology*. 2021;97(4):e378–e388. doi:10.1212/WNL.0000000000012228

49. Corsi–Cabrera M, Galindo–Vilchis L, del–Río–Portilla Y, Arce C, Ramos–Loyo J. Within–subject reliability and inter–session stability of EEG power and coherent activity in women evaluated monthly over nine months. *Clin Neurophysiol*. 2007;118(1):9–21. doi:10.1016/j.clinph.2006.08.013

50. Scally B, Burke MR, Bunce D, Delvenne JF. Resting–state EEG power and connectivity are associated with alpha peak frequency slowing in healthy aging. *Neurobiol Aging*. 2018;71:149–155. doi:10.1016/j.neurobiolaging.2018.07.004

51. van der Hiele K, Vein AA, Reijntjes RHAM, et al. EEG correlates in the spectrum of cognitive decline. *Clin Neurophysiol*. 2007;118(9):1931–1939. doi:10.1016/j.clinph.2007.05.070

52. Lashgari E, Liang D, Maoz U. Data augmentation for deep–learning–based electroencephalography. *J Neurosci Methods*. 2020;346:108885. doi:10.1016/j.jneumeth.2020.108885

53. Kwak NS, Müller KR, Lee SW. A convolutional neural network for steady state visual evoked potential classification under ambulatory environment. *PLOS ONE*. 2017;12(2):e0172578. doi:10.1371/journal.pone.0172578

54. Schirrmeister RT, Springenberg JT, Fiederer LDJ, et al. Deep learning with convolutional neural networks for EEG decoding and visualization. *Hum Brain Mapp*. 2017;38(11):5391–5420. doi:10.1002/hbm.23730

국문 초록

연구 배경: 단독 렘수면행동장애(iRBD) 환자는 알파-시누클레인병증의 전구 질환으로 80% 이상이 15년 이내에 파킨슨병(PD), 루이소체 치매(DLB), 다계통위축증(MSA)과 같은 신경퇴행성 질환으로 전환되는 것으로 잘 알려져 있다. 기준선 휴지기 뇌파는 알파-시누클레인병증 발병과 관련이 있는 것으로 보고되었다. 이 연구는 iRBD의 기준선에서 뇌파를 이용하여 알파-시누클레인병증 발병 시기 및 아형에 대한 예측 모델을 개발하는 것을 목표로 하였다.

연구 방법: 기준선에서 iRBD 환자에 대해 휴지기 뇌파 및 신경학적 평가를 수행하였다. 뇌파 스펙트럼 파워, 가중 위상 지연 지수, 새넌 엔트로피를 특징으로 사용하였다. PD-MSA 및 DLB 그룹에 대한 생존 예측을 위해 3개의 모델이 사용되었고 아형 예측을 위해 4개의 모델이 적용되었다. 또한 외부 검증을 수행하였다.

연구 결과: 233명의 환자를 최대 9년(평균 3.4년) 동안 추적 관찰했으며, 29명에서 알파-시누클레인병증이 발병하였다(PD 14명, DLB 9명, MSA 6명). 생존 예측을 위한 최상의 모델은 통합 브라이어 점수(IBS)가 0.113이고 우위성 지수(C-index)가 0.721인 Random survival forest 모델이었다. K-nearest neighbor 모델은 수신자 동작 특성 곡선 아래 면적이 0.908로 아형 예측 분석에 가장 적합한 모델이었다. 뇌파 감속과 관련된 기능은 두 모델 모두에서 높은 중요성을 보였다.

결론: 뇌파 바이오마커를 이용한 기계 학습 모델은 iRBD에서 알파-시누클레인병증 발병 시기 및 아형을 예측할 수 있다. 우리의 결과를 확증하기 위해서는 다양한 국가의 대규모 샘플 데이터를 포함한 추가 연구가 필요하다.

주요어 : 렘수면행동장애; 파킨슨병; 루이소체 치매; 다계통위축증; 뇌파; 기계 학습.
학 번 : 2020-25765